



Brazilian Journal of Physics

ISSN: 0103-9733

luizno.bjp@gmail.com

Sociedade Brasileira de Física

Brasil

Nasir Khattak, M.; Mushtaq, A.; Qamar, A.  
Ion Streaming Instabilities in Pair Ion Plasma and Localized Structure with Non-Thermal  
Electrons  
Brazilian Journal of Physics, vol. 45, núm. 6, 2015, pp. 633-642  
Sociedade Brasileira de Física  
São Paulo, Brasil

Available in: <http://www.redalyc.org/articulo.oa?id=46442560007>

- How to cite
- Complete issue
- More information about this article
- Journal's homepage in redalyc.org

redalyc.org

Scientific Information System

Network of Scientific Journals from Latin America, the Caribbean, Spain and Portugal

Non-profit academic project, developed under the open access initiative

# Ion Streaming Instabilities in Pair Ion Plasma and Localized Structure with Non-Thermal Electrons

M. Nasir Khattak<sup>1</sup> · A. Mushtaq<sup>2,3</sup> · A. Qamar<sup>1</sup>

Received: 12 June 2015 / Published online: 18 September 2015  
© Sociedade Brasileira de Física 2015

**Abstract** Pair ion plasma with a fraction of non-thermal electrons is considered. We investigate the effects of the streaming motion of ions on linear and nonlinear properties of unmagnetized, collisionless plasma by using the fluid model. A dispersion relation is derived, and the growth rate of streaming instabilities with effect of streaming motion of ions and non-thermal electrons is calculated. A quasi-potential approach is adopted to study the characteristics of ion acoustic solitons. An energy integral equation involving Sagdeev potential is derived during this process. The presence of the streaming term in the energy integral equation affects the structure of the solitary waves significantly along with non-thermal electrons. Possible application of the work to the space and laboratory plasmas are highlighted.

**Keywords** Pair ion plasma · Streaming instability · Solitary structure

## 1 Introduction

Pair plasma due to the equal mass of its constituent species presents a scenario where it is possible to avoid asymmetric

phenomena arising from large mass difference of plasma species. Although electron-positron pair plasmas make a good example of such plasmas and are of interest to physicists due to their natural occurrences, dense pair ion plasmas are more stable [1]. Moreover, recent successes in producing pair ion plasma (PI) in laboratory have also prompted the surge of activity in the field. The experimental configuration of hydrogen pair plasma ( $H^+$ ,  $H^-$ ) is presented in [2–4]. On the other hand, pair ion plasma are also relevant in astrophysical settings [5].

To explain the experimental results, it is suggested that pair ion plasma can contain a significant fraction of electrons. The experimental results of Oohara et al. also motivate the research on pair-ion-electron (p-i-e) plasma as it is expected that such plasma could also be produced in the laboratory. Therefore, linear and nonlinear wave structures are already investigated in such p-i-e plasma by several authors [6–8].

Streaming motion of plasma particles may become important in a variety of situations, e.g., in solar atmosphere [9, 10] and interstellar space [11], laser plasma interaction [12, 13], and in some space plasma phenomena [14]. The asymptotic study of the general solution of the dispersion relation reveals the linear two stream instabilities which are obtained in terms of three dimensionless parameters that characterize the steady state of the plasma. Such analysis determines (i) the analytical expression of the maximum growth rate and the associated wave number, (ii) the dominant different stability types of the parametric regions, (iii) the analytical expression for instability threshold, and (iv) the evolution in the character from one type to another type [15]. The well-known forms of two stream instabilities for electron ion (e-i) plasmas are the ion acoustic (IA) instability [16, 17] (for low drift velocities) and the Buneman or reactive instability [18] (for high drift velocities). A complete and systematic picture of different characteristics and types of linear streaming instabilities is presented in [19, 20].

✉ M. Nasir Khattak  
mnnasirphysics@gmail.com

<sup>1</sup> Department of Physics, University of Peshawar,  
25000 Peshawar, Pakistan

<sup>2</sup> Department of Physics, Abdul Wali Khan University Mardan,  
Mardan 23200, Pakistan

<sup>3</sup> National Center for Physics, Shahdrah Valley Road,  
Islamabad 44000, Pakistan

It is also interesting to study solitary structures in pair ion electron plasma. Both refractive and compressive solitons are observed at critical temperature of negative ions in [21]. Nakamura et al. [22] have studied the large amplitude solitary waves with negative ions in multicomponent plasma with experimental results of [22]. The linear and nonlinear behaviors of electrostatic waves in PI plasma are also investigated in [8, 17]. Some acoustic solitary waves and double layers with nonextensive, superthermal, and with non-thermal electrons are studied for both planar and non-planar geometry by Sahu et al. [23].

In this work, we investigate the effects of the streaming motion of ions on linear and nonlinear properties of pair ion plasma by using the plasma fluid model in unmagnetized, collisionless plasma, and the formation and properties of solitons. We derive the dispersion relation and calculate the growth rate of the instability. Doped pair ion plasma are supposed, which are not completely filtered, e.g., fullerene pair ion plasmas ( $C^{+60}$ ) with some fraction of electrons. The effect of non-thermal electrons on ion acoustic soliton in plasma with adiabatic positive and negative ions are considered. Quasi-potential approach is followed to study the characteristics of the ion acoustic solitons.

This manuscript is organized as follows. In Section 2, the basic equations and formulation of plasma dynamics are used to derive the dispersion relation for the growth rate of the streaming instability. In Section 3, we derive the growth rate of two stream instability for counter streaming ions and one stream instability for positive and negative ions. In Section 4, we derive the energy integral equation with Sagdeev potential which leads to the characteristics of soliton and solitary waves. The results and discussions are presented in Section 5 and summary and conclusion in Section 6.

## 2 Basic Equations and Formulation

We consider a PI plasma composed of positive and negative ions with non-thermal electrons. For instabilities analysis and to investigate the nonlinear dynamics of the solitary waves, we use the following one-dimensional hydrodynamic model given by the equation of motion and continuity equations for both positive and negative ions.

$$\frac{\partial n_j}{\partial t} + v_{j0} \frac{\partial n_j}{\partial x} + \frac{\partial(n_j v_j)}{\partial x} = 0 \quad (1)$$

$$\frac{\partial v_j}{\partial t} + v_{j0} \frac{\partial v_j}{\partial x} + \frac{1}{2} \frac{\partial v_j^2}{\partial x} \pm Z_j \frac{\partial \Phi}{\partial x} + \frac{3}{2} \delta_j \frac{\partial n_j}{\partial x} = 0 \quad (2)$$

The system is closed with the Poisson equation as

$$\frac{\partial^2 \phi}{\partial x^2} + n_+ - \mu n_e - (1-\mu)n_- = 0 \quad (3)$$

Where  $j$ =positive ion (+), negative ion (−) and  $n_j$  is the density of positive (negative) ion normalized by the background value  $n_{j0}$ , and  $v_j$  is the positive (negative) ion velocity normalized by ion acoustic speed  $C_s = (T_e/m_+)^{1/2}$  where  $T_e$  is the electron temperature and  $m_+$  is the mass of positive ion. The electrostatic wave potential  $\phi$  is normalized by  $k_B T_e / e$ . For adiabatic PI pressure, we have  $p_j = p_{j0} (n_j/n_{j0})^\gamma$ , where  $\gamma = \frac{N+2}{N}$ , is the polytropic index, with  $N$  being the number of degrees of freedom, and  $p_{j0} = n_{j0} K_B T_j$  is the equilibrium PI pressure. The ratio  $\delta_j = T_j/T_e$  represents the ions to electron temperature ratio. By using background quasi-neutrality, we have  $\mu = n_{e0}/n_{+0}$  and  $n_{-0}/n_{+0} = (1-\mu)$ . The time and space variables are normalized in terms of plasma period  $\omega_{p+}^{-1} = (m_j/4\pi n_{+0} Z_+ e^2)^{1/2}$ , and Debye length  $\lambda_{DE} = (T_e/4\pi n_{+0} Z_+ e^2)^{1/2}$  respectively. To describe the electron distribution with population of fast particles [24, 25], we take the following

$$f_e(v) = \frac{n_0}{(3\alpha + 1) + \sqrt{2\pi v_e^2}} \left( 1 + \frac{\alpha v^4}{v_e^4} \right) \exp\left(-\frac{v^2}{v_e^2}\right) \quad (4)$$

and integrating over the velocity space with dimensionless potential  $\phi$  gives the electron number density

$$n_e = n_{e0} e^{\phi} (1 - \beta \phi + \beta \phi^2) \quad (5)$$

Here,  $\beta = \frac{4\alpha}{1+3\alpha}$ , with  $\alpha$  being the parameter which determines the number of non-thermal electrons present in the non-thermal plasma model. Linearizing the number density with  $n_j = n_{j0} + n_{j1}$  and  $v_j = v_{j0} + v_{j1}$  representing  $n_{j1}$  and  $v_{j1}$  with dependence  $\exp(-i\omega t + ikx)$ , we obtain the following linearized equations

$$-(\omega - kv_{j0})n_{j1} + n_{j0}kv_{j1} = 0 \quad (6)$$

$$\frac{n_{j1}}{n_{j0}} = \pm \frac{k^2}{(\omega - kv_{j0})^2 - 3\delta_j n_{j0} k^2} \phi \quad (7)$$

$$-k^2 \phi = (1-\mu)n_{-1} + \mu n_{e1} - n_{+1} \quad (8)$$

and the linearized electron number density as

$$n_{e1} = 1 + \phi(1-\beta) \quad (9)$$

Using the Eqs. (6–9), the following dispersion relation is obtained

$$\frac{(1-\mu)}{[(\omega - kv_{-0})^2 - 3\delta_- k^2]} - \frac{(1-\beta)\mu}{k^2} + \frac{1}{(\omega - kv_{+0})^2 - 3\delta_+ k^2} = 1 \quad (10)$$

### 3 Instability Analysis

We now investigate the growth rate for one stream instability by using the parameter of cold ion, i.e.,  $v_{+0} = \delta_+ = 0$

$$1 = \frac{(1-\mu)}{(\omega - kv_{-0})^2 - 3\delta_- k^2} - \frac{(1-\beta)\mu}{k^2} + \frac{1}{\omega^2} \quad (11)$$

$$f(\omega) = \frac{(1-\mu)}{(\omega - kv_{-0})^2 - 3\delta_- k^2} - \frac{(1-\beta)\mu}{k^2} + \frac{1}{\omega^2} \quad (12)$$

where  $a = (1-\mu)$ ,  $\lambda = kv_{-0}$ ,  $b = \frac{(1-\beta)\mu}{k^2}$ , and  $c = \delta_- k^2$ . Instability occurs when Eq. (12) has complex roots. It occurs when the local minimum of  $f(\omega)$  for  $0 < \omega < (\pm 3c + \lambda)$  is greater than 1. The function  $f(\omega)$  is plotted against  $\omega$  in Fig. 1, for arbitrary values of  $a$ ,  $b$ ,  $c$ , and  $\lambda$ . The function  $f(\omega)$  has singularity at  $\omega = -1$ , and 2. For real and positive values of  $\omega$ , there are two propagating or stable regions separated by one non-propagating or unstable region.

#### 3.1 Instability Analysis by Carden's Method

Putting  $\omega = \omega_R + i\gamma$  in Eq. (11) and for plane waves analysis, the amplitude of the waves is either growing or damping. For growing instability  $\gamma > 0$  and for decaying waves  $\gamma < 0$ . Comparing the real and imaginary terms of  $\omega$ , we have

$$\gamma = \sqrt{A_1 \omega_R^2 + B_1 \omega_R - \frac{C_1}{\omega_R} - D_1} \quad (13)$$

$$A_2 \omega_R^3 + B_2 \omega_R^2 - C_2 \omega_R + D_2 = 0, \quad (14)$$

with  $A_1 = \frac{2kv_{-0}-1}{4kv_{-0}}$ ,  $B_1 = \frac{k[1+(1+\beta)(v_{-0}^2-3\delta_-)]}{4v_{-0}(1-\beta)}$ ,  $C_1 = \frac{k^3(v_{-0}^2-3\delta_-)}{4\mu v_{-0}(1-\beta)}$ ,  $D_1 = \frac{k^2}{2\mu(1-\beta)}$  and  $A_2 = \mu(1-\beta)$ ,  $B_2 = k\mu v_{-0} + (1-\beta)$ ,  $C_2 = k^2[\mu(v_{-0}^2-3\delta_-)(1-\beta)-1]$ ,  $D_2 = k^3 v_{-0}$ . The coefficients  $A_2$ ,  $B_2$ ,  $C_2$ ,  $D_2$  are all real, so the Eq. (14) has three real roots; we can then use these roots to reduce the cubic into quadratic equation. The Eq. (14) can be reduced to cubic without second degree term by the substitution  $\omega_R = Z - \frac{B_2}{3A_2}$ , and it reduces to

$$Z^3 + 3PZ + 2Q = 0, \quad (15)$$

where  $P = \frac{-C_2}{3A_2} - \frac{B_2^2}{9A_2^2}$  and  $Q = \frac{D_2}{2A_2} + \frac{C_2 B_2}{6A_2^2} + \frac{B_2^3}{27A_2^3}$ . By using the Carden's rule, the root of Eq. 15 can be written as

$$Z = \left[ \sqrt{P^2 + Q^2} - Q \right]^{\frac{1}{3}} - \left[ \sqrt{P^2 + Q^2} + Q \right]^{\frac{1}{3}} \quad (16)$$

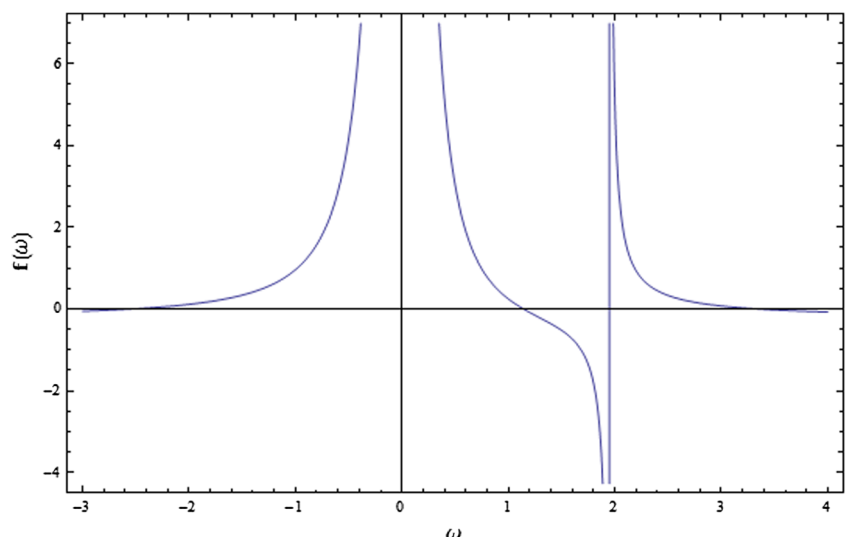
If we assume  $v_{-0} = 1$ ,  $\mu = 0.3$ ,  $\beta = 2$ ,  $\delta_- = 0.2$ , then  $P^3 + Q^2 < 0$ . The solution for  $Z$  is then

$$Z = -2\sqrt{-P} \cos \left[ \frac{1}{3} \arctan \left( \frac{\sqrt{-P^3 - Q^2}}{Q} \right) \right] \quad (17)$$

Using  $P$ ,  $Q$  and  $Z = \omega_R + \frac{B_2}{3A_2}$  in (17), we then determine the root of  $\omega_R$  as

$$\omega_R = -\frac{B_2}{3A_2} - 2\sqrt{\frac{C_2}{3A_2} + \frac{B_2^2}{9A_2^2}} \cos \left[ \frac{1}{3} \arctan \left( \frac{\sqrt{\left( \frac{C_2}{3A_2} + \frac{B_2^2}{9A_2^2} \right)^3 - \left( \frac{D_2}{2A_2} + \frac{C_2 B_2}{6A_2^2} + \frac{B_2^3}{27A_2^3} \right)^2}}{\frac{D_2}{2A_2} + \frac{C_2 B_2}{6A_2^2} + \frac{B_2^3}{27A_2^3}} \right) \right] \quad (18)$$

**Fig. 1** Sketch of  $f(\omega)$  as a function of  $\omega$  using Eq. (12). The arbitrary parameters used are  $\lambda = 1$ ,  $a = 0.5$ ,  $b = 0.2$ , and  $c = 0.3$



Now the growth rate for streaming instability in pair-ion plasma in this special case can be written as

$$\gamma = \sqrt{\frac{2k-1}{4k}\omega_R^2 + 0.15k\omega_R - \frac{0.333k^3}{\omega_R} - 1.666k^2} \quad (19)$$

Similarly, if we consider the negative ions as cold and at rest (i.e.,  $v_{-0}=\delta_-=0$ ) species, we will have the similar results as of (18) and (19) for real and growth rate of the instability, but when positive ions are streaming. These results show how an increase in free energy of the plasma which is given by the stream of the beams of ions leads to instabilities. This increase in the free energy is responsible for plasma to be unstable. The instabilities do not arise without free energy. The free energy may come from anisotropic plasma pressure or streaming of plasma particles with respect to each other. Here, in these cases, the free energy is due to streaming of ions.

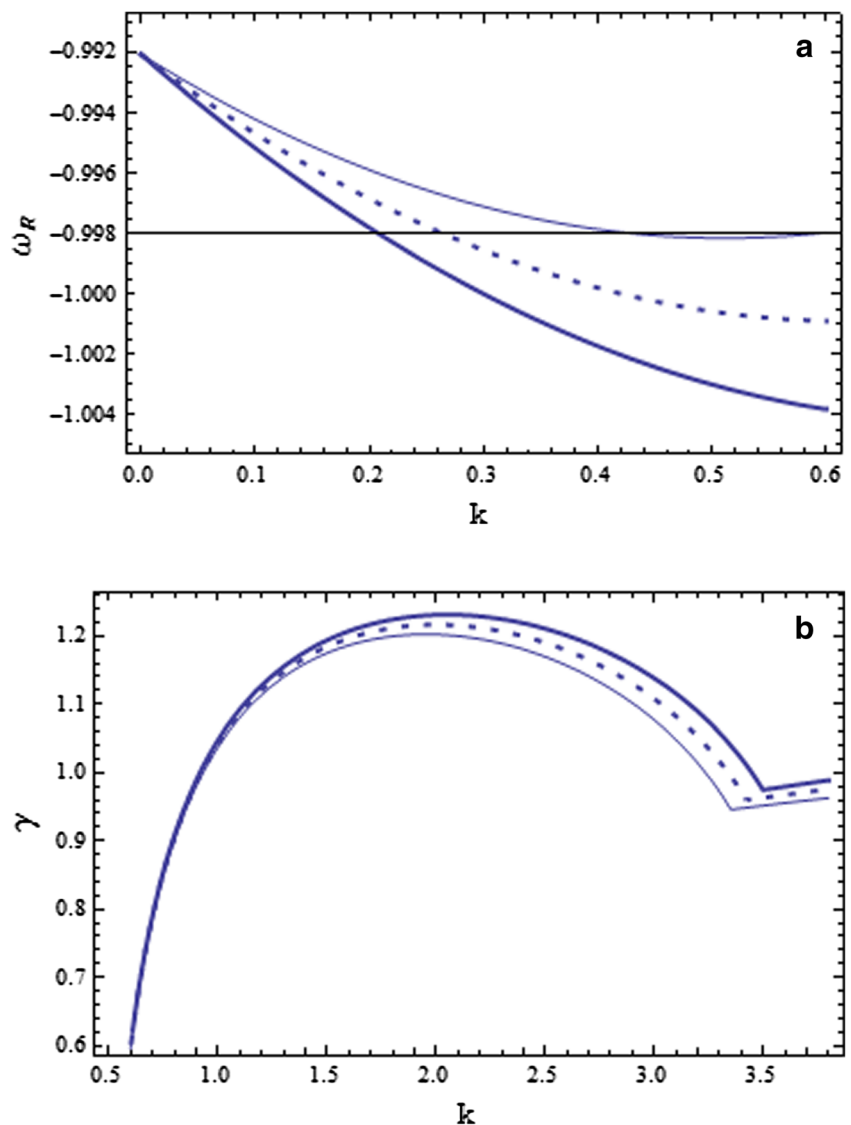
**Fig. 2** Sketches of **a**  $\omega_R$  and **b** growth rate  $\gamma$  as a function of wave vector  $k$  for different values of  $v_{-0}$ . Using Eqs. (18) and (19), such that  $v_{-0}=1$  (solid line),  $=1.2$  (dotted line), and  $=1.4$  (bold line). Other parameters are  $\mu=0.012$ ,  $\delta_+=0.2$ ,  $\delta_-=0.1$ , and  $\beta=0.5$

#### 4 Formulation of Energy Integral Equation

We adopt the pseudo-potential approach for examining the existence and properties of solitary structures. It is useful to use the moving frame of reference  $\xi=x-Mt$  where  $M=u/c_s$  is the Mach number and  $u$  is the speed of the localized nonlinear structure moving with the frame. Solving together (1) and (2) with boundary conditions  $n_{\pm} \rightarrow 1$ ,  $v_{\pm} \rightarrow 0$ ,  $\phi \rightarrow 0$  at  $\xi \rightarrow \pm\infty$ , we obtain a general solution for PI in terms of  $n_{\pm}^2$  as

$$n_{\pm}^2 = \frac{1}{2\delta_{\pm}} \left[ \chi_{\pm} + \sqrt{\chi_{\pm}^2 - 12\delta_{\pm}M_{D\pm}^2} \right] \quad (20)$$

where  $\chi_{\pm} = M_{D\pm}^2 + 3\delta_{\pm} \mp 2Z_{\pm}\phi$  with  $M_{D\pm} = M - v_{\pm 0}$  is the Doppler Mach number. Following the idea of [24–26], we look for solution  $n_{\pm}$  in the form



$$n_{\pm} = \frac{1}{\sqrt{2}} \left[ \sqrt{X} \pm \sqrt{Y} \right] \quad (21)$$

Using (20) in (21) will allow us to determine  $X$  and  $Y$  as

$$X = \frac{1}{6\delta_{\pm}} \left[ \left( M_{D\pm} + \sqrt{3\delta_{\pm}} \right)^2 \mp 2Z_{\pm}\phi \right] \quad (22)$$

$$Y = \frac{1}{6\delta_{\pm}} \left[ \left( M_{D\pm} - \sqrt{3\delta_{\pm}} \right)^2 \mp 2Z_{\pm}\phi \right] \quad (23)$$

Using (22) and (23) and after some standard algebraic manipulation leads to the following expressions for  $n_{+}$  and  $n_{-}$

$$n_{+} = \frac{1}{2\sqrt{3\delta_{+}}} \left[ \left( M_{D+} + \sqrt{3\delta_{+}} \right)^2 - 2Z_{+}\phi \right]^{\frac{1}{2}} \pm \left[ \left( M_{D+} - \sqrt{3\delta_{+}} \right)^2 - 2Z_{+}\phi \right]^{\frac{1}{2}} \quad (24)$$

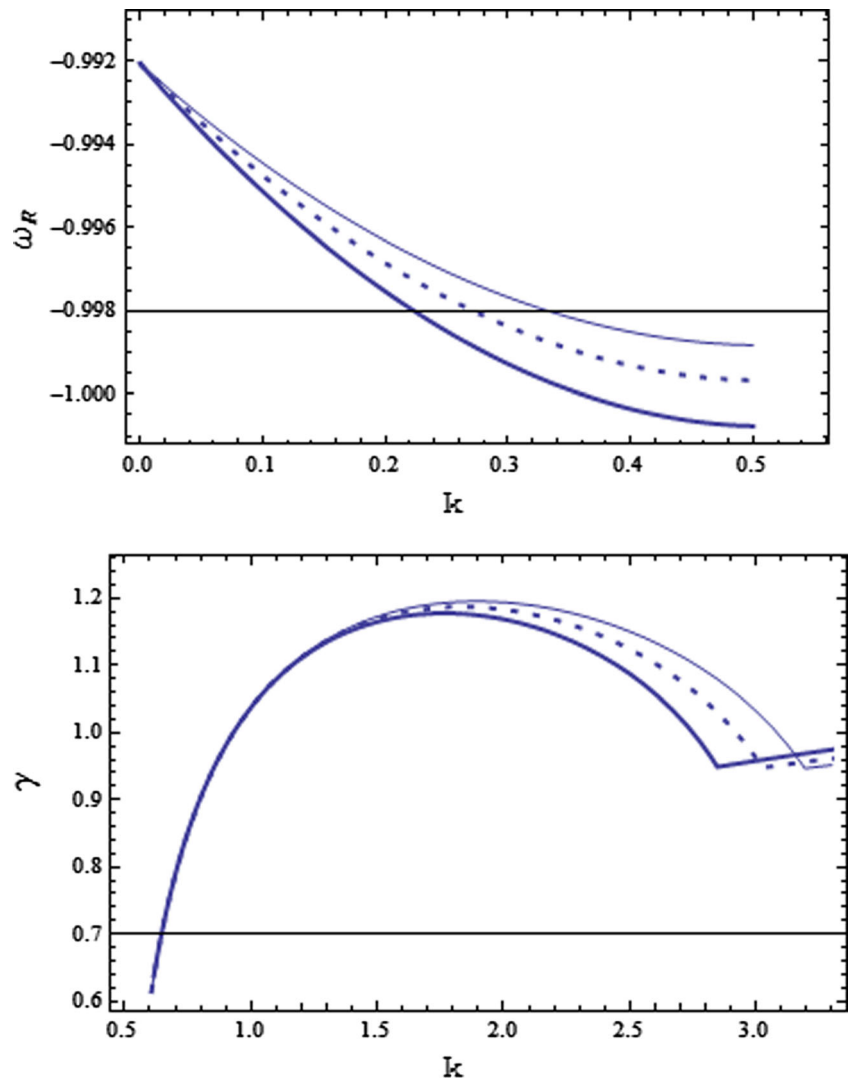
$$n_{-} = \frac{1}{2\sqrt{3\delta_{-}}} \left[ \left( M_{D-} + \sqrt{3\delta_{-}} \right)^2 + 2Z_{-}\phi \right]^{\frac{1}{2}} \pm \left[ \left( M_{D-} - \sqrt{3\delta_{-}} \right)^2 + 2Z_{-}\phi \right]^{\frac{1}{2}} \quad (25)$$

Employing all the constituent densities from (9), (24), and (25) into (3), after multiplication by  $\frac{d\phi}{d\xi}$  and integration, leads to the energy integral equation as

$$\frac{1}{2} \left( \frac{d\phi}{d\xi} \right)^2 + V(\phi) = 0, \quad (26)$$

where  $V(\phi)$  is the pseudo-potential (or Sagdeev potential), which can be expressed as

**Fig. 3** Variation of growth rate  $\gamma$  as a function of  $k$  for different values of nonthermality of electrons  $\beta$ , using Eq. (19), such that  $\beta=0.55$  for solid curve,  $\beta=0.6$  for dashed curve, and  $\beta=0.65$  for bold solid curve. Other parameters are  $\mu=0.012$ ,  $\delta_{+}=0.2$ ,  $\delta_{-}=0.1$ , and  $v_{-o}=1$



$$\begin{aligned}
V(\phi) = & \mu \left[ 1 + 3\beta e^{-\phi} + 3\beta e^{\phi}(\phi-1) - \beta\phi^2 e^{\phi} \right] \\
& + \frac{1}{6\sqrt{3\delta_+}} \left[ \left( M_{D+} + \sqrt{3\delta_+} \right)^3 \pm \left( M_{D+} - \sqrt{3\delta_+} \right)^3 \right] \\
& - \frac{1}{6\sqrt{3\delta_+}} \left\{ \left[ \left( M_{D+} + \sqrt{3\delta_+} \right)^2 - 2_{z+\phi} \right]^{\frac{3}{2}} \pm \left[ \left( M_{D+} - \sqrt{3\delta_+} \right)^2 - 2_{z+\phi} \right]^{\frac{3}{2}} \right\} \\
& + \frac{(1-\mu)}{6\sqrt{3\delta_-}} \left[ \left( M_{D-} + \sqrt{3\delta_-} \right)^3 \pm \left( M_{D-} - \sqrt{3\delta_-} \right)^3 \right] \\
& - \frac{(1-\mu)}{6\sqrt{3\delta_-}} \left\{ \left[ \left( M_{D-} + \sqrt{3\delta_-} \right)^2 + 2_{z-\phi} \right]^{\frac{3}{2}} \pm \left[ \left( M_{D-} - \sqrt{3\delta_-} \right)^2 + 2_{z-\phi} \right]^{\frac{3}{2}} \right\}
\end{aligned} \quad (27)$$

Now for isothermal electrons ( $\beta \rightarrow 0$ ), the Sagdeev potential (27) can be modified as

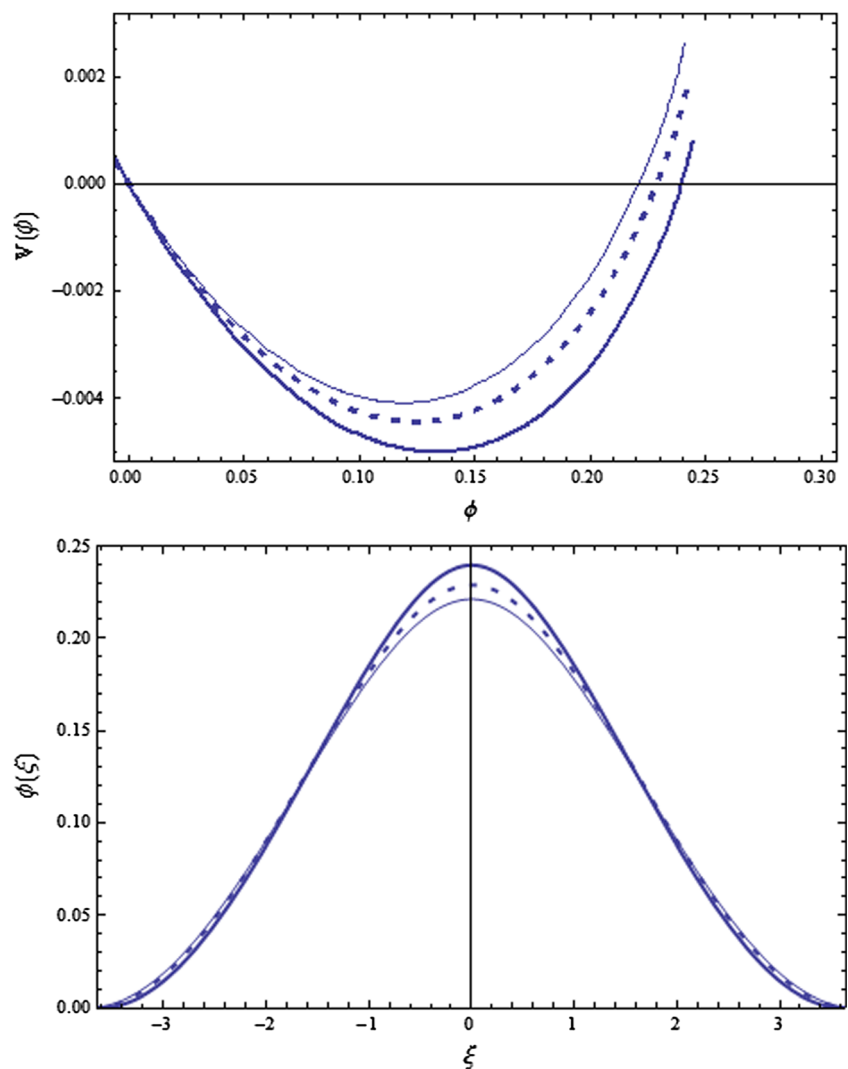
$$\begin{aligned}
V(\phi) = & \mu [1 - e^{-\phi}] \\
& + \frac{1}{6\sqrt{3\delta_+}} \left[ \left( M_{D+} + \sqrt{3\delta_+} \right)^3 \pm \left( M_{D+} - \sqrt{3\delta_+} \right)^3 \right] \\
& - \frac{1}{6\sqrt{3\delta_+}} \left\{ \left[ \left( M_{D+} + \sqrt{3\delta_+} \right)^2 - 2_{z+\phi} \right]^{\frac{3}{2}} \pm \left[ \left( M_{D+} - \sqrt{3\delta_+} \right)^2 - 2_{z+\phi} \right]^{\frac{3}{2}} \right\} \\
& + \frac{(1-\mu)}{6\sqrt{3\delta_-}} \left[ \left( M_{D-} + \sqrt{3\delta_-} \right)^3 \pm \left( M_{D-} - \sqrt{3\delta_-} \right)^3 \right] \\
& - \frac{(1-\mu)}{6\sqrt{3\delta_-}} \left\{ \left[ \left( M_{D-} + \sqrt{3\delta_-} \right)^2 + 2_{z-\phi} \right]^{\frac{3}{2}} \pm \left[ \left( M_{D-} - \sqrt{3\delta_-} \right)^2 + 2_{z-\phi} \right]^{\frac{3}{2}} \right\}
\end{aligned} \quad (28)$$

**Fig. 4** Behavior of the Sagdeev potential  $V(\phi)$  against  $\phi$  (*upper panel*) and the corresponding soliton profile (*lower panel*) for different values of positive ion streaming  $v_{+o}$  such that  $v_{+o}=0.02$  (*solid line*),  $=0.022$  (*dotted line*), and  $=0.025$  (*bold line*). Other physical parameters used are  $\mu=0.012$ ,  $\delta_+=0.2$ ,  $\delta_-=0.1$ ,  $\beta=0.5$ ,  $v_{-o}=0.01$ , and  $M=0.1$

Equation (27) can be regarded as an “energy integral equation” of an oscillating particle of unit mass, with pseudo-speed  $\frac{d\phi}{d\xi}$ , pseudo-position  $\phi$ , pseudo-time  $\xi$ , and pseudo-potential  $V(\phi)$ . The form of pseudo-potential could determine whether the solitary wave or soliton of (27) exists or not. It is clear that  $V(\phi)=0$  and  $\frac{dV(\phi)}{d\phi}=0$  at  $\phi=0$ . In this case, solitary wave structure exists if  $\frac{d^2V(\phi)}{d\phi^2} \leq 0$  at  $\phi=0$  so that zero as a fixed point is unstable. All the specified conditions are satisfied. Besides that,  $V(\phi)$  should be negative between  $\phi=0$  and  $\phi_m$ , where  $\phi_m$  is the maximum (or minimum) value of  $\phi$ . The second condition is known as soliton condition. It is seen that for lower sign from (27), we have

$$\frac{\partial^2 V(M)}{\partial \phi^2} = (\beta - \mu) + \frac{Z_+}{M_{D+}^2 - 3\delta_+} - \frac{(1-\mu)Z_-}{M_{D-}^2 - 3\delta_-} < 0 \quad (29)$$

For  $v_{+0}=v_{-0}=v_0$ , which implies that  $M_{D+}=M_{D-}=M_D$ , then Eq. (29) can be treated as a quadratic in  $M_D^2$ . By





considering  $M=M_s$  at  $\frac{\partial^2 V(M)}{\partial \phi^2} = 0$ , we then get the following relation

$$M^2 > M_s^2 = v_0 + \frac{b}{2a} \left[ 1 + \left( 1 - \frac{4ac}{b^2} \right)^{\frac{1}{2}} \right] \quad (30)$$

where  $a=\mu(\beta-1)$ ,  $b=3\mu(\beta-1)(\delta_++\delta_-)-\mu$  and  $c=9\mu(\beta-1)\delta_+\delta_- - 3\delta_- - 3(1-\mu)\delta_+$ . Equation (30) gives the lower limit for  $M$  in the presence of non-thermal electrons, which corresponds to the true IA velocity in the given plasma model.

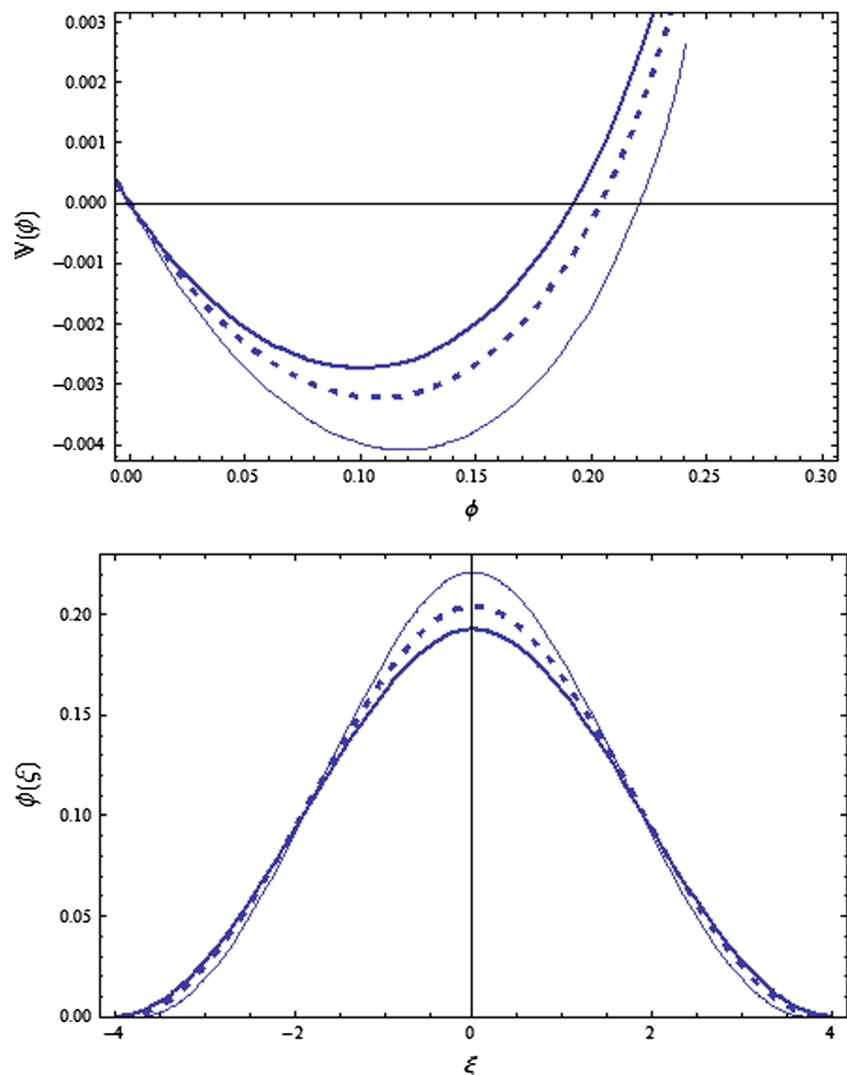
## 5 Results and Discussions

For numerical evaluation of the growth rates and real frequencies  $\omega_R$ , we choose some typical parameters that are representative of some laboratory plasmas [2, 3].  $n_e \simeq 10^7 \text{ cm}^{-3}$ ,  $n_{\pm} \simeq (10^7 - 10^{10}) \text{ cm}^{-3}$ ,  $T_e \sim 2 \text{ eV}$  and  $T_{\pm} \sim (0.13 - 0.16) \text{ eV}$ ,  $\mu = 0.6$ ,  $\beta = 1.18$ ,  $\delta_+ = 0.3$ ,  $\delta_- = 0.2$ , and for some arbitrary values of

$v_{\pm o}$ . Using these parameters, we solved Eqs. (13–19) numerically and examined the effects of ions streaming and nonthermality of electrons on ion acoustic waves.

Real frequency  $\omega_R$  and growth rate variations with  $k$  were computationally analyzed from Eqs. (18–19) for various values of plasma parameters. Figure 2a shows the dispersion relation (18) for negative ions streaming. The plot is drawn for the root of  $\omega_R$  as a function of wave vector  $k$  for different values of  $v_{-o}$ . It shows that for increasing values of  $v_{-o}$ , the real frequency  $\omega_R$  decreases with decreasing trend against  $k$ . While on the other hand, growth rate increases for increasing values of  $v_{-o}$  as shown in Fig. 2b. Which means that due to streams of ions, the ion acoustic waves grow exponentially and causes instability. Figure 3 indicates variation of growth rate as a function of  $k$ , for different values of nonthermality of electrons  $\beta$ . It shows the growth rate  $\gamma$  decreases with increased values of  $\beta$ . It predicts that nonthermality is stabilizing the given mode in the system.

**Fig. 5** Behavior of the Sagdeev potential  $V(\phi)$  against  $\phi$  (upper panel) and the corresponding soliton profile against  $\xi$  (lower panel) for different values of negative ion streaming  $v_{-o}$  such that  $v_{-o} = 0.01$  (solid line),  $= 0.005$  (dotted line), and  $= 0.018$  (bold line). All the other parameters are the same as in Fig. 4 with  $v_{-o} = 0.02$





Now to examine the existence regions and nature of IA solitary waves excitation with streaming motion of ions in PI plasma, the numerical solutions of Eqs. (26–27) have been analyzed using the above-mentioned typical plasma parameters. The effects of ions streaming ( $v_{\pm o}$ ), ions temperature ( $\delta_{\pm}$ ), nonthermality ( $\beta$ ), and concentration of electrons on the behavior of IA solitary waves are displayed in Figs. 4, 5, and 6. These results shows that our present plasma model gives the compressive soliton.

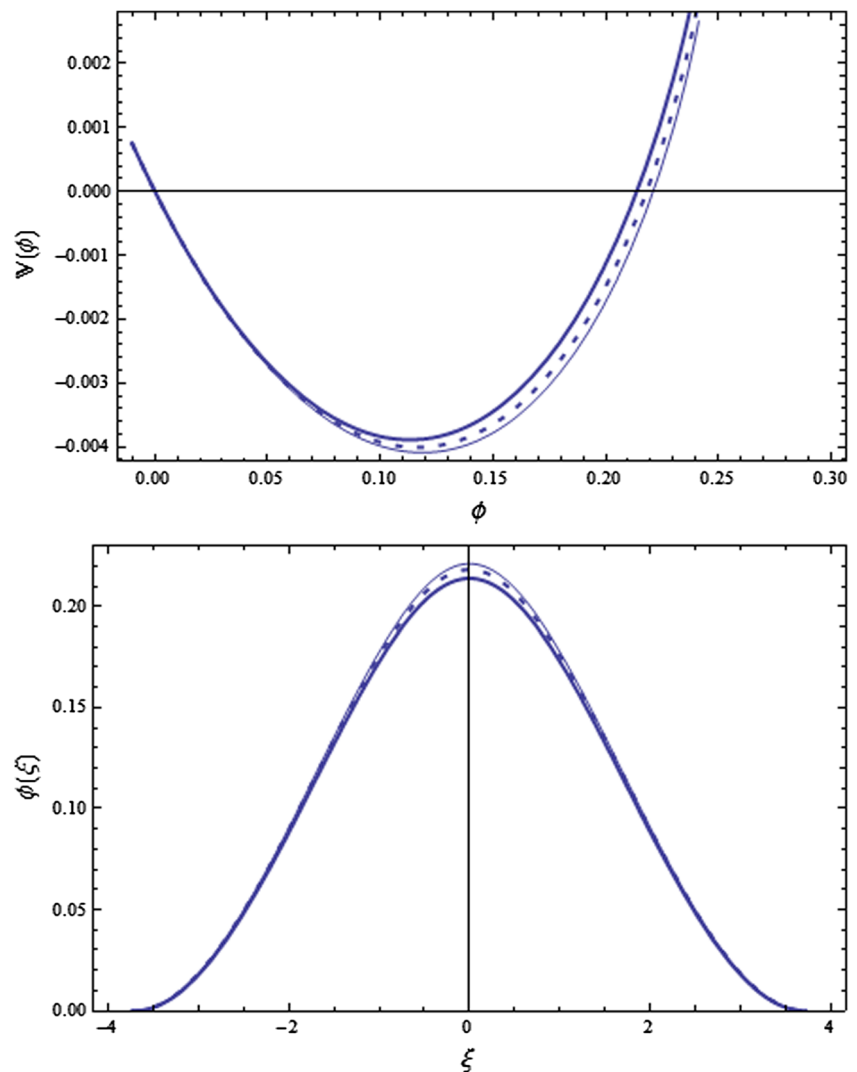
The Sagdeev potential curves and the corresponding solitary wave profiles for different values of positive ion streaming  $v_{+o}$  are plotted in Fig. 4. It is observed from the upper panel of Fig. 4 that increased values of  $v_{+o}$  increases the depth of the Sagdeev potential on the positive  $\phi$ -axis. The corresponding solitary waves with higher amplitude with respect to  $v_{+o}$  is shown in the lower panel of Fig. 4. It means that the positive ion streaming is playing the role of energizing the soliton profile. While on the other hand, the negative ion streaming is de-

energizing the soliton profile, with decreased Sagdeev potential well and with lower soliton amplitude as shown in Fig. 5 (upper and lower panel respectively). Streaming of ions are the sources of free energy but the negative ion streaming is like the sink for soliton formation in order to make the system conservative.

The Sagdeev potential curves and the corresponding solitary wave profiles for various values of nonthermality of electrons  $\beta$  are drawn in Fig. 6. It is found from the upper panel of Fig. 6 that the profile depth of the Sagdeev potential decreases with  $\beta$  on the positive  $\phi$ -axis. The corresponding solitary waves with lower amplitude with increased values of  $\beta$  are shown in the lower panel of Fig. 6. This entails that the nonthermality of electrons is de-energizing the soliton, in the presence of streaming ions. But the effect of deactivation is not that much significant for given  $\beta$  values, as obvious from the figure.

The increased value of electron concentration ( $\mu$ ) decreases the depth of Sagdeev potential and correspondingly enhances the amplitude of solitary waves. This is respectively shown in

**Fig. 6** Sagdeev potential  $V(\phi)$  (upper panel) as a function of electrostatic potential  $\phi$  (lower panel) and the corresponding soliton profile as a function of  $\xi$  (lower panel) for various values of nonthermality of electrons  $\beta$ , such that  $\beta=0.5$  (solid line),  $=1.5$  (dotted line), and  $=3$  (bold line). All the other parameters are the same as in Figs. 4 and 5



the upper and lower panel of Fig. 7. The increased value of  $\mu$  raises electron thermal energy. Since ion acoustic waves are pressure-driven waves, so the higher values of electron thermal energy will definitely increase the height and will decrease the width of solitons.

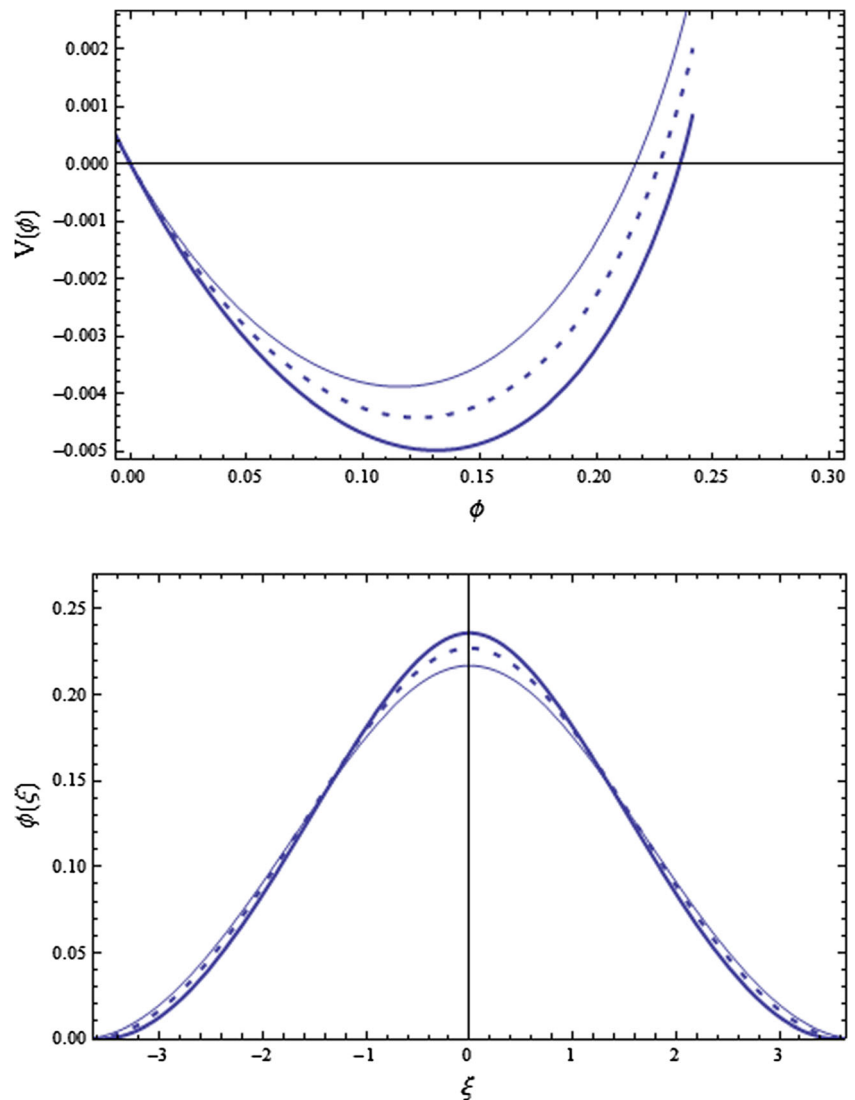
## 6 Conclusion

To summarize, the results show how an increase in free energy of the plasma which is given by the stream of the beams of ions leads to perturbations. Due to these beams, perturbations waves are growing and instabilities called streaming instabilities occur. We have studied the positive and negative ions streamings in PI plasmas in the presence of non-thermal electrons. From these streaming instabilities, the knowledge of growth rates has been presented here. The motion of the positive ion beam is the source of free energy, if it is not supported continuously, the instability quenches itself after the beam has

slowed down to certain threshold which is determined by the background particles. We have studied the growth rates as a function of wave vector, and as the growth rates increase the instabilities enhance otherwise damping of wave occurs. It has been shown that growth rate decreases with  $\beta$ .

We have also studied the effects of ions streaming ( $v_{\pm o}$ ), ions temperature ( $\delta_{\pm}$ ), nonthermality ( $\beta$ ), and concentration of electrons on the behavior of IA solitary waves in PI-electron plasma. The electrons are assumed to follow a distribution with a population of fast particles [27, 28]. The solitary waves exist because of the counterbalance between nonlinearity induced due to the streaming motion and the dispersion due to the temperature effects. Using pseudo-potential approach, we have derived an energy integral equation involving Sagdeev potential. The presence of the streaming term in the energy integral equation affects the structure of the solitary waves significantly. It has been shown that positive and negative ions streamings are acting opposite to each other on soliton profile. Also, it has been observed that nonthermality of electrons is

**Fig. 7** Effect of electron concentration ( $\mu$ ) on Sagdeev potential (*upper panel*) and soliton (*lower panel*) such that  $\mu=0.01$  (*solid line*),  $=0.015$  (*dotted line*), and  $=0.02$  (*bold line*). All the other parameters are the same as in Figs. 4 and 5



de-energizing the soliton. In the present case, our analysis has shown compressive soliton, where positive ions play a dominating role in its formation. Our present results should be useful in understanding the wave phenomena and associated nonlinear electrostatic structures in the laboratory pair ion electron plasmas.

## References

1. E.P. Liang, S.C. Wilks, M. Tabak, Phys. Rev. Lett. **81**, 4887 (1998)
2. W. Oohara, R. Hatakeyama, Phys. Rev. Lett. **91**, 205005 (2003)
3. W. Oohara, Y. Kawabara, R. Hatakeyama, Phys. Rev. E **75**, 056403 (2007)
4. W. Oohara, R. Hatakeyama, Phys. Rev. Lett. **95**, 175003 (2005)
5. J. Hedin, M. Rapp, J. Gumbel, I. Strelnikova, M. Friedrich, F.J. Lubken, Geophys. Res. Lett. **32**, 123821 (2005)
6. R. Saeed, A. Mushtaq, Phys. Plasmas **16**, 032307 (2009)
7. B. Zhao, J. Zheng, Phys. Plasmas **15**, 082314 (2008)
8. A. Mushtaq, M. Nasir Khattak, Z. Ahmad, A. Qamar, Phys. Plasmas **19**, 042304 (2012)
9. G.R. Magelssen, D.F. Smith, Sol. Phys. **55**, 211 (1977)
10. J.B. Zirker, O. Engvold, S.F. Martin, Nature **396**, 440 (1998)
11. E. Fermi, Phys. Rev. **75**, 1169 (1949)
12. D.N. Gupta, K.P. Singh, A.K. Sharma, N.K. Jaiman, Phys. Plasmas **11**, 5250 (2004)
13. S. Kumar, H.K. Malik, Phys. Scr. **74**, 304 (2006)
14. T. Obayashi, Space Sci. Rev. **3**, 79 (1963)
15. E.A. Jackson, Phys. Fluids **3**, 786 (1960)
16. N.A. Krall, A.W. Trivelpiece, *Principles of Plasma Physics* (McGraw-Hill, New York, 1973)
17. O. Buneman, Phys. Rev. **115**, 503 (1959)
18. D.B. Melrose, *Instabilities in Space and Laboratory Plasmas* (Cambridge University Press, New York, 1986)
19. V. Lapureta, E. Ahedo, Phys. Plasmas **9**, 5 (2002)
20. Y. Nakamura, I. Tsukabayashi, Phys. Rev. Lett. **52**, 2356 (1984)
21. Y. Nakamura, I. Tsukabayashi, J. Plasma Phys. **34**, 401 (1985)
22. H. Saleem, P.K. Shukla, B. Eliasson, Phys. Scr. **77**, 015503 (2008)
23. B. Sahu, R. Roychoudhury, Phys. Plasmas **12**, 052106 (2005)
24. F. Verheest, M.A. Hellberg, I. Kourakis, Phys. Plasmas **15**, 112309 (2008)
25. S.S. Ghosh, K.K. Ghosh, A.N.S. Lyengar, Phys. Plasmas **3**, 3939 (1998)
26. T.K. Baluku, M.A. Hellberg, I. Kourakis, N.S. Saini, Phys. Plasmas **17**, 053702 (2010)
27. R.A. Cairns, A.A. Mamun, R. Bingham, R. Bostrom, R.O. Dendy, C.M.C. Nairn, P.K. Shukla, Geophys. Res. Lett. **22**, 2709 (1995)
28. R.A. Cairns, R. Bingham, R.O. Dendy, C.M.C. Nairn, P.K. Shukla, A.A. Mamun, J. Phys. IV **5**, C6–43 (1995)